

# Comparisons of the PTB primary clocks with TAI in 1999

A. Bauch, B. Fischer, T. Heindorff, P. Hetzel,  
G. Petit, R. Schröder and P. Wolf

**Abstract.** The primary clocks CS1, CS2 and CS3 of the Physikalisch-Technische Bundesanstalt (PTB) have contributed to the realization of International Atomic Time, TAI (Temps Atomique International), throughout 1999. Their operation, their performance and the uncertainty with which they realized the International System of Units (SI) second are described in some detail, together with the results and associated uncertainties of comparisons of the realized second with the TAI scale unit for each clock.

## 1. Introduction

Terrestrial Time (TT) has been defined by the International Astronomical Union as a coordinate time for the geocentric reference system, such that its scale interval agrees with the SI second on the geoid. International Atomic Time is a realization of TT, apart from a constant offset in time. The realization of TAI is based on the Free Atomic Time Scale, EAL (Échelle Atomique Libre) computed at the Bureau International des Poids et Mesures (BIPM) as a weighted average of data obtained from about 210 atomic clocks – mainly commercial caesium clocks and a few hydrogen masers. A linear function of time is added to EAL with the slope adjusted in order to generate TAI as an international time reference conforming to the above definition. This so-called steering of TAI is based on comparisons between EAL and a few primary frequency standards (PFSs) that are operated in national metrology institutes and which realize the SI second with a specified uncertainty [1, 2]. Thus *the results of comparisons of primary frequency standards are essential for establishing the accuracy of TAI and ensuring traceability to the SI second.* The italicized phrase is taken from Recommendation S 3 which, among others, was adopted at the 14th Meeting of the Consultative Committee for Time and Frequency (CCTF) in March 1999 [3]. It was recommended that the results of the PFS comparisons should be published

in more detail than commonly practised. Until recently, a single line of data for each month or for each time interval during which the standard was operated was published in *Circular T*, issued by the BIPM Time Section, and later published in the Annual Report of the Section. This practice was thought not to fulfil users' needs. In particular the uncertainty,  $u$ , with which the user of the data can access the SI second as given by a particular clock, should be given explicitly for a specified time interval together with the necessary information to allow the user to estimate the total uncertainty when combining such intervals or using subintervals. The information provided to the user should therefore contain the following components:

- $u_B$ , reflecting the combined uncertainty from systematic effects;
- $u_A$ , originating in the instability of the PFS;
- $u_{\text{link/lab}}$ , reflecting the link between the PFS and the clock whose data are communicated to the BIPM and processed in the ALGOS formalism;
- $u_{\text{clock-TAI}}$ , reflecting the uncertainty in the link to TAI of this contributing clock;
- information on the instability  $\sigma_{\text{TAI}}(\tau)$  of TAI itself.

In addition, the statement of the uncertainty components which are then combined to give the total uncertainty  $u$  should follow the rules laid down in the ISO *Guide to the Expression of Uncertainty in Measurement* [4] as far as applicable. This paper has been written in fulfilment of these recommendations.

At the PTB, PFSs have been operated since 1969 when the CS1 came into existence [5, 6]. The CS2 was finished in the mid-1980s and has been operated until today without major interruption [7]. Development of the CS3 and CS4 primary clocks has been under way

A. Bauch, B. Fischer, T. Heindorff, P. Hetzel and R. Schröder:  
Physikalisch-Technische Bundesanstalt (PTB): POB 3345,  
D-38023 Braunschweig, Germany.  
e-mail: time@ptb.de

G. Petit and P. Wolf: Time Section, Bureau International des  
Poids et Mesures (BIPM), Pavillon de Breteuil, F-92312  
Sèvres, France.

for some time: the CS3 clock became operational in 1995, and the CS4 is still under development. During 1999, CS1, CS2, and CS3 contributed to the realization of TAI. The PTB has continued to realize two atomic time scales. As has been the practice since 1991, the free atomic time scale TA(PTB) is based on the output of the CS2. The PTB coordinated universal time scale, UTC(PTB), differed from TA(PTB) only by a constant time offset until 1 January 1998. A time step of +1900 ns was then introduced to UTC(PTB) and frequency steering was started. This steering is carried out on a monthly basis with rate changes equal to  $\pm 0.5$  ns/day, if necessary. The steering corrections are published in the PTB *Time Service Bulletin*.

This paper is organized as follows. First, the mode of operation of the devices and the methods of obtaining and communicating their results are laid down. Section 3 deals with the observed frequency instability of the PFSs during 1999, based on data obtained at the PTB, which demonstrate their short-term behaviour, and on the results of comparison with TAI. The  $u_A$  components have been derived from these data. A discussion follows of the uncertainty contributed by the time transfer method employed to link the PFS to EAL and TAI, respectively, together with information on TAI instability. Detailed descriptions of how the clocks' uncertainties  $u_B$  were evaluated have been published for the CS3 [8] and more recently for the rebuilt CS1 [6]. No such refereed publication exists as yet for the CS2, therefore Section 5 explains the evaluation of the uncertainty  $u_B$  with particular emphasis on the CS2. To sum up, Section 6 discusses the results on the deviation of the duration of the TAI scale interval from the SI second as realized by the individual clocks with the associated uncertainty for 1999. The paper concludes with some remarks on ongoing research at the PTB and future developments.

## 2. Operation of PTB PFSs

CS1, CS2 and CS3 operate as clocks in the common meaning of the word. In each clock a quartz oscillator in a control loop is the physical source of a 5 MHz signal used for frequency comparisons and of a pulse-per-second (1 pps) signal  $T(clock)$  which is continuously compared with UTC(PTB). The environmental conditions, the performance of the clocks' hardware and the understanding of the underlying physics are not static. Operational parameters thus have to be regularly checked and validated if the uncertainty of the clock is to be known for any given period. This is illustrated in the following.

The magnetic field strength in the clock is determined from measurements of the Zeeman frequency and the microwave power level is determined from the response of the atoms at resonance. Both quantities are manually adjusted to the appropriate level, if necessary. Linewidth measurements give the mean atomic velocity,

and the correction for the quadratic Doppler effect is applied according to the measurement results. These measurements are performed during "normal" servicing, typically once or twice per week. The spectral purity of the microwave excitation signal and a few signals in the electronics are recorded much less frequently, sufficiently to monitor the proper functioning of the equipment. Usually this is done on the occasion of a beam reversal, about once every 10 to 14 weeks. Beam reversals have been performed on all clocks in 1999, as discussed below. For this to take place, the positions of oven and detector at each end of the clock have to be interchanged. Clock operation of the CS1 has to be interrupted for about 8 hours whereas only 30 minutes are needed for this action on the CS2 and the CS3. After each beam reversal, the strength of the magnetic quantization field (C-field) has to be changed by about 1 part in  $10^3$ , as explained in detail in [6].

Of course, the quartz control loop has to be opened during such service work. In order to avoid a loss of coherence in the 5 MHz signal and the occurrence of a time step, the quartz oscillator is phase-locked during the servicing work to an external 5 MHz signal whose frequency deviates by less than 2 parts in  $10^{14}$  from that of the primary clock. The accumulated time error in this slaved mode is thus below 100 ps during the period required for "normal" servicing work. If the interruption lasts longer, such as after a CS1 beam reversal, the time difference  $[UTC(PTB) - T(clock)]$  is reset to the predicted value with a precision of 100 ps. Following this practice, a continuous time scale is obtained from each clock.

Figure 1 illustrates the generation of UTC(PTB) and the time interval measurement set-up. Time difference values  $[UTC(PTB) - T(clock)]$  obtained at 0:00 UTC of the days with the Modified Julian Day (MJD) ending in 4 and 9 are reported to the BIPM. This constitutes the basis of the clocks' contribution to TAI, together with the routinely performed GPS common-view time comparisons between UTC(PTB) and UTC(OP), maintained by the BNM-LPTF (Bureau National de Métrologie, Laboratoire Primaire du Temps et des Fréquences, France). Section 4 gives details of the stability of the measurements at the PTB and the link to TAI.

The CS1 was operated through most of 1999. Since August 1999, however, the CS1 was employed for an experimental verification of the so-called Ramsey pulling frequency shift (see below). Clock data have thus not been useful for processing by the BIPM. The CS2 was in service without interruption and without major modifications being made. In the CS3, which is operated with vertical atomic beams in contrast to the CS1 and the CS2, new detector supply electronics for the lower detector were successfully installed in early summer 1999. When the same action was taken on the upper detector a failure occurred in the current-to-voltage converter, which is housed inside the main

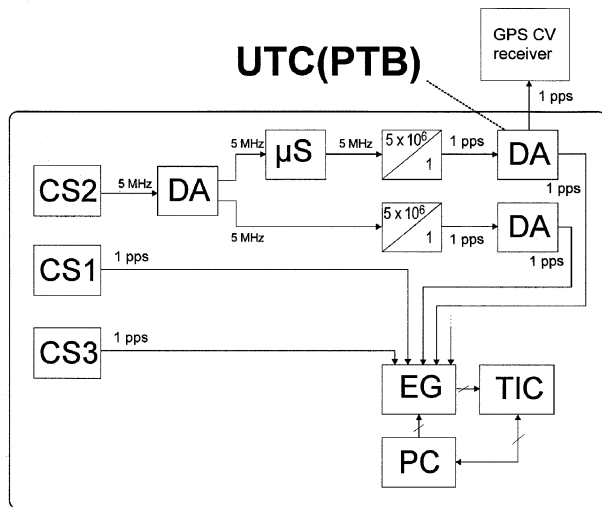


**Figure 1.** Realization of UTC(PTB) based on the signal of the CS2 throughout 1999, and the 1 pps measurement set-up employed for clock comparisons. DA: distribution amplifier;  $\mu$ S: microphase stepper; EG: electronic gates; TIC: time interval counter. All equipment within the box is operated inside the PTB temperature-stabilized clock hall, where the ambient temperature is about 23.4 °C with peak-to-peak variations of 0.4 °C throughout the year under normal conditions.

vacuum chamber. Thus for the last months of 1999 only the up-down beam could be operated. Clock operation was stopped on 30 November to perform the necessary repair.

### 3. Frequency instability component, $u_A$

As the PTB clocks are operated continuously (in the sense defined above) their contribution to the realization of TAI is based on monthly comparisons, i.e. 30-day averages. In principle the frequency instability of the clocks should be known for each of the 30-day intervals. In practice the instability is estimated by analysing their performance over an extended period and obtaining average values for the required intervals.

The short-term frequency instability of the clocks for averaging times up to  $\tau = 12$  h was evaluated several times throughout 1999 by comparison with one of the PTB active hydrogen masers. 5 MHz signals were compared in a high-resolution phase comparator which allows the clocks' frequency instability to be determined for all averaging times  $\tau$  without contributing significant measurement noise. On the other hand, the frequency instability, expressed by the classical Allan standard deviation  $\sigma_y$ , was predicted, based on the clocks' atomic line-quality factor, the clock transition signal, shot noise and thermal detector noise, as given in Table 1. In the case of the CS1, the total beam signal and, even more so, the ratio of clock transition signal divided by total beam signal, have slightly decreased with time. A range of values is therefore given in the table. In the case of the CS2, the signals differ for the two atomic beams

**Table 1.** Relative frequency instability expressed by the non-overlapping Allan standard deviation  $\sigma_y$  ( $\tau = 1$  h) of the PTB primary clocks CS1, CS2, and CS3; predicted and measurement values. Figures in curly brackets represent the  $1\sigma$  uncertainty for the estimate of  $\sigma_y$ , which follows from the limited number of observations.

| Clock | $\sigma_y$ ( $\tau = 1$ h)<br>predicted                      | $\sigma_y$ ( $\tau = 1$ h)<br>measurement value  |
|-------|--|--|
| CS1   | $(87 \text{ to } 99) \times 10^{-15}$                        | $(84 \text{ to } 103) \times 10^{-15}$   |
| CS2   | beam 1: $60 \times 10^{-15}$<br>beam 2: $67 \times 10^{-15}$ | $57 \times 10^{-15}$ , $\{3 \times 10^{-15}\}$<br>$72 \times 10^{-15}$ , $\{3 \times 10^{-15}\}$   |
| CS3   | $122 \times 10^{-15}$  | $217 \times 10^{-15}$ , $\{28 \times 10^{-15}\}$<br>$126 \times 10^{-15}$ , $\{6 \times 10^{-15}\}$<br>(before and after replacement<br>of detector electronics) |

so two values are reported in the table. In the case of the CS3, for many years the frequency instability has significantly exceeded the predicted value. Only in 1999, after the replacement of the detector supply electronics, did the agreement become much better, as reflected in the two values given.

If the frequency instability is dictated by white frequency noise originating entirely from beam shot noise and thermal detector noise, the expectation values for  $\sigma_y$  are about  $93 \times 10^{-15} (\tau/h)^{-1/2}$ ,  $63 \times 10^{-15} (\tau/h)^{-1/2}$  and  $122 \times 10^{-15} (\tau/h)^{-1/2}$  for CS1, CS2 and CS3, respectively. A previous three-cornered-hat analysis of clock comparison data, taken between May 1997 and May 1999, yielded Allan deviations  $\sigma_y$  ( $\tau = 30$  d) of  $5.1 \times 10^{-15}$ ,  $2.4 \times 10^{-15}$  and  $7.1 \times 10^{-15}$  for CS1, CS2, and CS3, respectively, showing slightly excessive instability for CS1 and CS3. As the CS1 had not been operated normally since August 1999 and because operation of the CS3 with improved instability lasted only 4 months, no other data were available at the time of writing.

From a GPS CV frequency comparison between the CS2 and the UTC scale of the United States Naval Observatory, UTC(USNO),  $\sigma_y$  ( $\tau = 30$  d) =  $3.5 \times 10^{-15}$  was obtained for the interval MJD 51180 to MJD 51540. The instability due to the link is probably dominated by systematic effects (such as hardware variations) estimated to be of the order of  $\sigma_{tt}(30 \text{ d}) \approx 1 \times 10^{-15}$  (see Section 4). The  $3.5 \times 10^{-15}$  quoted above is the combined instability of the comparison. The discrepancy with respect to the other values can be explained by taking into account the link instability and the instability of UTC(USNO).

Figure 2 shows the results of comparisons between the individual clocks and TAI as taken from *Circular T* (issues 133 to 144). The grey points represent CS1 data which were not used by the BIPM but which are still useful for estimating the instability of the comparison. The relative standard deviations of the twelve values around their respective mean value amount to  $0.48 \times 10^{-14}$ ,  $0.32 \times 10^{-14}$  and  $0.82 \times 10^{-14}$  for the CS1, CS2 and CS3, respectively. In summary, the values found from the three-cornered-hat analysis

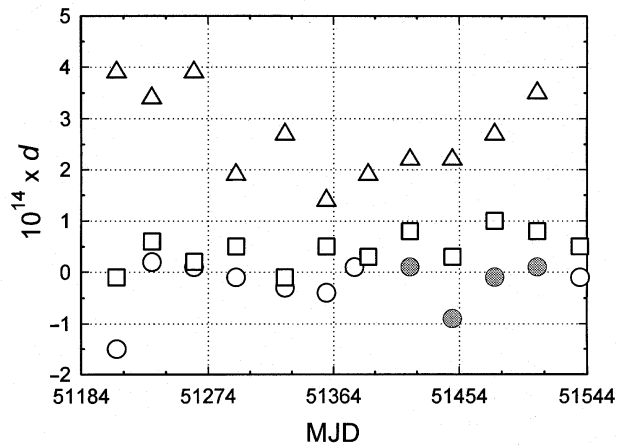


**Figure 2.** Fractional deviation,  $d$ , of the duration of the TAI scale interval from the SI second as realized by the individual clocks CS1 (○), CS2 (□) and CS3 (△) during 1999. The CS1 data indicated in grey were taken while the experiments were performed (see Section 5) and were not used by the BIPM. MJD denotes Modified Julian Day; MJD 51544 corresponds to 2000-01-01.

are to our knowledge best suited to express the  $u_A$  contribution and are thus included in Table 5 (Section 6).

#### 4. Time interval measurements at PTB, link between PTB and TAI, TAI instability

Time interval measurements are performed under computer control with a Stanford Instruments SR620 time interval counter once per hour. The measurement channel  $[UTC(PTB) - T(CS2)]$  serves as a practical routine control of the performance of the equipment (see Figure 1). The rate difference is realized by a TST1040 microphase stepper. Figure 3a shows time difference data for December 1999 and Figure 3b shows a time instability plot. The noise observed in the data is a combination of the pure measurement noise – in fact only about 25 ps for a single shot measurement – and the additional phase wander which is probably introduced by the microphase stepper. The term  $u_{\text{link/lab}}$ , mentioned in the Introduction, is thus negligibly small compared with the instability of the external link, discussed subsequently.

The time transfer between UTC(PTB) and TAI was provided in 1999 by GPS common-view with UTC(OP) maintained by the BNM-LPTF in Paris. In turn UTC(OP) is linked to all laboratories participating in TAI through one or two GPS links. For a laboratory  $k$  in Europe, only one link is used. For a laboratory  $k$  outside Europe, an additional intercontinental GPS link is used, mostly independent of the European link. An estimate follows of the fractional frequency instability arising from time transfer noise for the two types of link considered above:  $[UTC(PTB) - UTC(OP)]$  and an intercontinental link. Each value may be considered as the sum of two components: measurement noise,

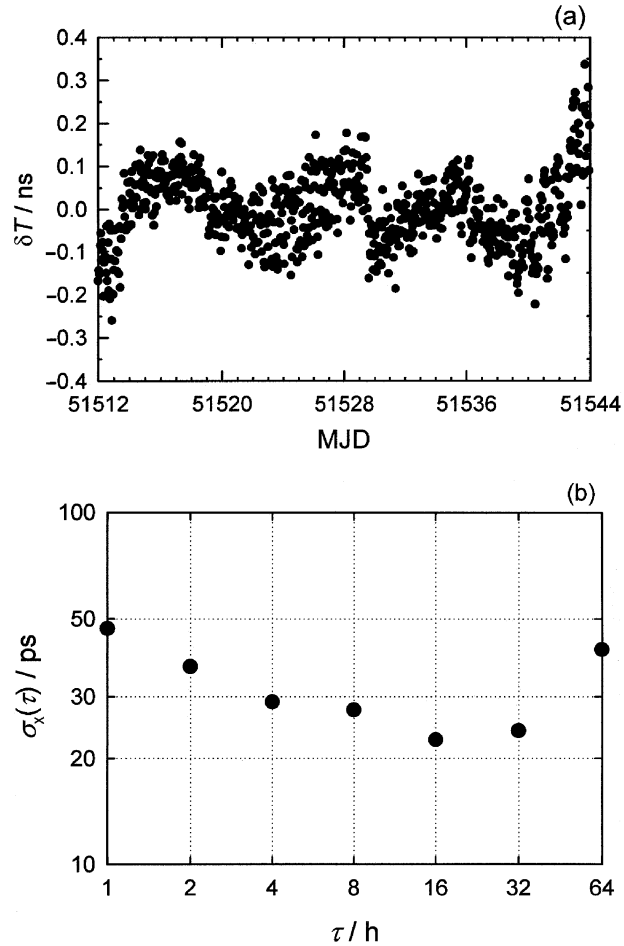


**Figure 3.** Example of local clock comparison performance, obtained during December 1999: (a) de-trended time differences  $[UTC(PTB) - T(CS2)]$  taken each full hour; (b) time instability  $\sigma_x(\tau)$  for the period under study. The short-term jitter can be identified as white-phase measurement noise. The wander is probably caused by the microphase stepper used in the generation of UTC(PTB) (see Figure 1).

denoted  $\sigma_m(\tau)$ , which is considered as white phase noise that can be reduced by averaging, and the noise arising from slowly varying effects such as the sensitivity of hardware delays to the environment,  $\sigma_s(\tau)$ . The combined value represents the uncertainty  $u_{\text{clock-TAI}}$  in the link to TAI.

The contribution  $\sigma_m(\tau)$  may be estimated from the expected time variance (TVAR),  $\sigma_x$ , of a single GPS CV measurement and their average spacing,  $\tau_0$ :  $\sigma_m(\tau) = \sqrt{3(\sigma_x/\tau_0)(\tau/\tau_0)^{-3/2}}$ . For both types of link considered above,  $\tau_0$  is estimated to be 2 ns.  $\tau_0$  is of order 2500 s for the PTB-OP link, while it is of the order of 5000 s for an intercontinental link. The resulting measurement noise for a 30-day average is about  $\sigma_m(\tau = 30 \text{ d}) = 4 \times 10^{-17}$  for the PTB-OP link and about  $\sigma_m(\tau = 30 \text{ d}) = 6 \times 10^{-17}$  for an intercontinental link.

Several studies may help with the task of estimating  $\sigma_s(\tau)$ . One is a 500-day comparison of the three

**Table 2.** Relative frequency corrections applied in routine operation of the PTB primary clocks CS1, CS2 and CS3. Where necessary, two values for each entry are given, valid for the two beam directions.

| Cause of frequency shift                        | CS1  | CS2  | CS3  |
|---|--|--|--|
| Magnetic field<br>(quadratic Zeeman shift)      | $-3.1784 \times 10^{-10}$<br>$-3.1722 \times 10^{-10}$ | $-3.1778 \times 10^{-10}$<br>$-3.1728 \times 10^{-10}$ | $-2.7735 \times 10^{-10}$<br>$-2.7727 \times 10^{-10}$ |
| Time dilation<br>(quadratic Doppler effect)     | $5.1 \times 10^{-14}$                                  | $4.8 \times 10^{-14}$<br>$5.0 \times 10^{-14}$         | $2.8 \times 10^{-14}$<br>$2.7 \times 10^{-14}$         |
| Cavity phase difference                         | $+3.1 \times 10^{-13}$<br>$-3.1 \times 10^{-13}$       | $+2.5 \times 10^{-13}$<br>$-2.6 \times 10^{-13}$       | $+4 \times 10^{-14}$<br>$-4 \times 10^{-14}$           |
| Gravitational potential<br>(height above geoid) | $8.7 \times 10^{-15}$                                  | $8.7 \times 10^{-15}$                                  | $8.7 \times 10^{-15}$                                  |

different links between the PTB and USNO realized with independent techniques [9]. The *Circular T* data (GPS CV technique) are compared with GPS carrier phase results (GeTT technique), and GeTT is itself compared with the Two-Way Time and Frequency Transfer (TWSTFT) technique. For both comparisons, the peak-to-peak variations have an amplitude of about 10 ns. Similarly, *Circular T* data (GPS CV technique) have been compared with TWSTFT for the PTB-NIST link over 7 months, yielding a modified Allan deviation of the difference,  $\text{mod } \sigma_y(\tau = 30 \text{ d})$ , of  $6 \times 10^{-16}$ . Information on  $\sigma_s(\tau)$  may also be inferred from the repeatability of a series of GPS calibration trips, aimed at determining the calibration delays of GPS receivers, the results of which are collected at the BIPM. For the comparison between the PTB and OP receivers, five calibration trips were conducted between 1994 and 1998 and four results are consistent within 3 ns, one result being out by 10 ns, the standard uncertainty of each result being stated as 2 ns or 3 ns. As such measurements tend to represent possible long-term (years) variations of the delays, this only allows us to infer that the possible effect of such long-term variations over 30 days may be limited to about 1 ns. From these results, a reasonable value such as  $u_{\text{clock-TAI}}(\tau = 30 \text{ d}) \approx 1 \times 10^{-15}$  may be inferred.

The instability  $\sigma_{\text{TAI}}(\tau)$  of TAI has been estimated for the period January 1997 to February 1999 using a five-cornered-hat analysis with four of the best atomic time scales. The resulting TAI instability can be modelled conservatively by three noise components:

- a white frequency noise  $6 \times 10^{-15}/(\tau/\text{d})$ ;
- a flicker frequency noise  $0.6 \times 10^{-15}$ ;
- a random-walk frequency noise  $0.16 \times 10^{-16} \times \sqrt{(\tau/\text{d})}$ .

### 5. Combined uncertainty from systematic effects, $u_B$

The total uncertainty of a time interval measurement with a primary clock specifies to what extent the measurement may deviate from the value of that interval in ideal SI seconds. The uncertainty is composed of two components, one linked to the instability of the clock over that interval (which is generally dependent on

the length of the interval) and the other to systematic effects,  $u_B$  (usually independent of the length of the interval). The distinction between these two components is fundamental. In reality it is also possible to make this distinction because the contributions to  $u_B$  can to a large extent be evaluated by means that are independent of the clock instability. The individual contributions are considered to be linearly independent. The standard uncertainty  $u_B$  is thus obtained as the square root of the sum of squares of the individual contributions. The CS1 relative frequency uncertainty has been evaluated as  $7 \times 10^{-15}$  ( $1 \sigma$ ), as laid down in [6]. The CS2 uncertainty has been evaluated as  $12 \times 10^{-15}$  ( $1 \sigma$ ), the main references for which are [7, 10, 11]. The value reported here, however, is based on a critical review of previous publications and experience gained in the meantime. The CS3 uncertainty has been evaluated as  $14 \times 10^{-15}$  ( $1 \sigma$ ), and the evaluation is the subject of [8]. The performance of the CS3 has not fully confirmed the validity of this estimate as in the past relative frequency excursions up to twice the uncertainty have been observed. In 1999 the clock behaved rather well, but the systematic offset noticeable in Figure 2 is still a matter of concern.

Table 2 gives the values for the individual corrections applied in routine operation of the clocks. The table contains the corrections owing to the height of the clocks above the geoid that are applied in order to realize the SI second as if the clocks were operated on the geoid. Note that corrections for the frequency shift arising from black-body radiation are not applied during operation. The frequency shifts were evaluated and communicated to the BIPM Time Section and are reported below. Table 3 lists the individual uncertainty components, most of which have previously been communicated. Deviations from these values, which have to be allowed for because of disturbed operation for certain periods in 1999, are explained under individual subheadings.

#### 5.1 Magnetic field – quadratic Zeeman effect

The presence of the C-field in the interaction region increases the clock transition frequency (zero field value  $f_0 = 9\,192\,631\,770 \text{ Hz}$ ) by about 3 Hz. The determination of the relative frequency correction  $F_C$

**Table 3.** Contributions to the relative uncertainty,  $u_B$ , in parts in  $10^{15}$  of the primary clocks CS1, CS2 and CS3. References are given in the text.

| Cause of frequency shift                           | CS1 | CS2 | CS3 |
|--|-----|-----|-----|
| Magnetic field                                     | 1   | 5   | 7   |
| Electric field of thermal radiation (Stark effect) | 1   | 1   | 1   |
| Time dilation (quadratic Doppler effect)           | 0.5 | 1   | 1   |
| Majorana transitions                               | 2   | 3   | 2   |
| Ramsey pulling                                     | 3   | 3   | 3   |
| Asymmetry of microwave spectrum                    | 0.2 | 0.2 | 0.5 |
| Cavity phase difference                            | 6   | 10  | 10  |
| Cavity detuning                                    | 0.3 | 0.1 | 0.2 |
| Electronics  | 1   | 1   | 1   |

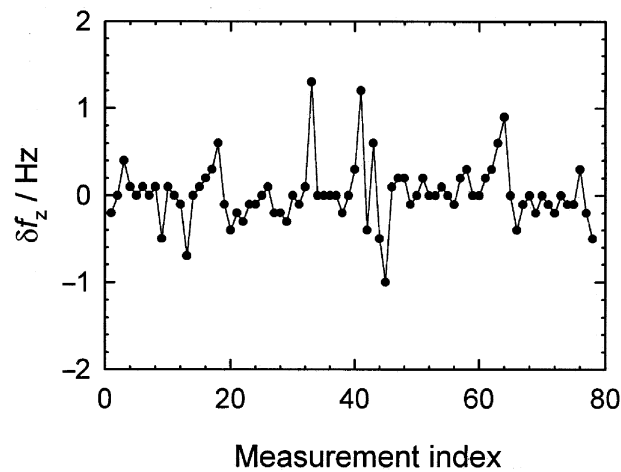


**Figure 4.** Measured deviation,  $\delta f_z$ , between actual and nominal value of the Zeeman frequency  $f_z$  in the CS2 during 1999. Measurements were taken once or twice a week. A deviation  $\delta f_z = 1$  Hz would indicate that in the preceding time interval the clock frequency was potentially in error by 1 part in  $10^{14}$ .

comprises measurements of the mean C-field strength and its inhomogeneity. The determination of the inhomogeneity has been documented for the CS1 [6], the CS2 [11] and the CS3 [8] and has not been repeated in 1999. The figures reported in Table 3 can still be taken as conservative estimates of this uncertainty contribution. Type A contributions to the uncertainty were determined by repeated determinations of  $f_z$ , the frequency separation between the (4,1)-(3,1) and (4,0)-(3,0) transition lines, which is a measure of the mean C-field strength. Knowing  $f_z$ ,  $F_C$  is computed according to  $F_C = -8(f_z/f_0)^2(1 + f_z/f_0)$ . As an example, Figure 4 shows the results of  $f_z$  measurements with the CS2 throughout 1999, plotted as a time series. The maximum deviation (for 30-day averages) between measurement and target values amounts to 0.25 Hz. This translates to an additional uncertainty of  $\delta F_C = 16f_z\delta f_z/f_0^2 = 3 \times 10^{-15}$ .

The same type of analysis was carried out for the CS1 and the CS3. For the CS1, the field instability

was found to be lower, while for the CS3 it was higher:  $-0.16$  Hz and  $0.5$  Hz, respectively. During interval G (MJD 51359 to MJD 51389) of Table 5 the temperature control system in the PTB clock hall failed occasionally and it cannot be excluded that large  $f_z$  variations have remained undetected. Therefore for this particular period the uncertainty component is taken as three times its normal value.

### 5.2 Electric fields – Stark effect

The electric fields of thermal radiation emitted from the surface of the enclosure produce a significant frequency shift due to the ac Stark effect,  $f_{acS}$ . According to [12], which contains the latest measurement results of the dc Stark effect, the clock transition frequency is shifted by  $f_{acS} = -1.573(3) \times 10^{-4} \text{ Hz } (T/300 \text{ K})^4 \times [1 + 0.014 (T/300 \text{ K})^2]$  in the presence of thermal radiation from a perfect black body at temperature  $T$ . The effect was not considered to be serious when clocks CS2 and CS3 were assembled, and thus temperature measurement on the vacuum enclosure was not regarded as necessary. The estimate of the frequency shift and its uncertainty was only made in 1995 and communicated to the BIPM; it is repeated here.

#### 5.2.1 CS1

The evaluation is described in [6]. The frequency correction due to the ac Stark effect is estimated based on  $T_{CS1} = 297.2(5)$  K and amounts to  $17.0(5) \times 10^{-15}$  ( $1 \sigma$  uncertainties in parentheses).

#### 5.2.2 CS2

The CS2 has a two-stage vacuum system with the inner vacuum tank, in which UHV conditions are maintained, being included in a tank in which a pressure of about 0.5 mPa is maintained. No direct temperature measurement has ever been made on the surface of the inner vacuum tank, which dictates the intensity of thermal radiation seen by the atoms. At the same time the tank serves as the support of the coil producing the magnetic quantization field. Its temperature is slightly higher than ambient temperature, as shown by the following observation. When at one end of the CS2 the caesium oven is heated from ambient temperature to its normal operational temperature, a change in the mean strength of the magnetic field is noticed which can be explained by a thermal expansion of the coil corresponding to a 1 K temperature rise. In normal operation of the clock, thermal radiation should thus be produced by a surface at 2 K above ambient temperature. Heat conduction probably takes place towards the ends connected to the vacuum chambers containing the ovens and detectors, which introduces uncertainty arising from unknown temperature gradients. Thus, the relative frequency

correction due to the ac Stark effect is estimated based on  $T_{\text{CS2}} = 299(2)$  K and amounts to  $17(1) \times 10^{-15}$  (1  $\sigma$  uncertainties in parentheses).

### 5.2.3 CS3

A Pt-100  $\Omega$  resistor is mounted in the middle of the vacuum chamber on its outer surface. With both ovens at operational temperature and all electronic equipment, which is mounted close to the clock's case, in operation, the temperature is about 6 K above ambient temperature. The relative frequency shift is estimated based on  $T_{\text{CS3}} = 305(2)$  K and amounts to  $18(1) \times 10^{-15}$ .

Theoretical studies have been made on all three clocks to establish to what extent the radiation present along the atomic beam may deviate from perfect black-body radiation characterized by the temperature of the surroundings. The uncertainty has been estimated accordingly.

### 5.3 Time dilation – relativistic Doppler effect

Special relativity predicts that time dilation causes the clock frequency observed in the laboratory frame to shift by  $f_{\text{D}} \approx -v^2/(2c^2)f_0$ , compared with the eigenfrequency in the rest frame,  $f_0$ , of the atoms when they move with velocity  $v$  in the clock. The linewidth of the central Ramsey fringe and, in more detail, the full recorded Ramsey pattern contains information to deduce  $v$  and the distribution of velocities of atoms contributing to the clock transition signal [6, 13]. The Ramsey pattern exhibits its first minimum transition probability next to the central fringe at a frequency separation  $W'$ , which is almost equal to the linewidth  $W$  (frequency separation between the two points on the central fringe with half-maximum transition probability). During clock operation, servicing includes a measurement of  $W'$ , which is a good measurement quantity and more easily accessible than  $W$  itself. An unambiguous relation between  $F_{\text{D}}$  and  $W'$  exists for fixed measurement conditions,  $F_{\text{D}} = k_{\text{clock}}(W'/\text{Hz})^2$ :  $k_{\text{CS1}} = 1.3 \times 10^{-17}$  [6],  $k_{\text{CS3}} = 1.4 \times 10^{-17}$  [13]. Following the procedures described in [6],  $k_{\text{CS2}} = k_{\text{CS3}}$  was found, which is unsurprising as both clocks have microwave cavities of the same length, slightly longer than that in the CS1. In 1999, nineteen measurements of  $W'$  were documented for the CS1, eight for the CS2 and five for the CS3. In the CS1,  $W'$  decreased steadily throughout the year from 62.9 Hz to 62.3 Hz. There may be a common cause of this phenomenon and the observed change in total beam signal and clock transition amplitude. It is thought that part of the polarizer magnet bore becomes more and more obstructed with caesium compounds forming on the surface under the rather poor vacuum conditions in the CS1 oven chamber. The CS2 and CS3 measurement results varied only within the measurement uncertainty of 0.05 Hz, confirming the findings of previous years.

### 5.4 Cavity phase difference

The evaluation of the related frequency shift by beam reversals has been a major issue in previous papers and is not repeated here. Information is included in [6, 14] for the CS1, in [11] for the CS2 and in [8] for the CS3. The uncertainty components reported in Table 3 are valid if the uncertainty with which a beam retrace can be performed remains unchanged. This cannot be validated without dismantling the clock. In addition, it has to be assumed that the properties of the cavity remain unchanged despite its years of exposure to caesium. This would be even more difficult to verify. In this context it may be useful to note the temporal evolution of the beam reversal frequency shift,  $F_{\text{BR}}$ , for the clocks, which has been archived for many years. Figures 5a, 5b and 5c show the results for the three clocks. Each of the data points represents the relative difference of frequency values taken before and after a beam reversal. Measurements were made with respect to reference clocks and typically averaged over 2 weeks (for the CS1) and 10 days (for the CS2 and the CS3).

In the case of the CS1, the primary clock CS2, three commercial high-performance caesium clocks, two hydrogen masers and, if data were available, the time scales UTC(NIST), UTC(USNO) and UTC(NPL) were used to determine  $F_{\text{BR}}(\text{CS1})$ . The standard deviation of the individual values around the mean of  $-622 \times 10^{-15}$  is  $8 \times 10^{-15}$ . The short-term frequency instability of the CS1 would alone predict  $8 \times 10^{-15}$ . Figure 5a may be misleading in that a systematic upward trend in  $F_{\text{BR}}(\text{CS1})$  could be suspected. But, as explained in [6], the mode of operation of the CS1 was changed around MJD 50690 in such a way that a small change in  $F_{\text{BR}}$  could indeed be expected. A linear fit to points from MJD 50720 onwards shows no statistically significant slope and it is tempting to say that the end-to-end phase difference  $\phi$  of the CS1 cavity was stable during that period. No beam reversal in the CS1 was carried out after May 1999, as the CS1 was used for studies of the Ramsey pulling frequency shift (see below).

In the case of the CS2, international references were used only from 1997. However, the apparent improvement in the stability of  $F_{\text{BR}}(\text{CS2})$  cannot be entirely explained by this change in procedure. In 1996 and 1997 some improvements were made in the CS2 hardware. Shielding of microwave leakage was improved and dc ground loops were removed. In fact, none of these measures were expected to have any impact on the determination of  $F_{\text{BR}}(\text{CS2})$ . For the twelve data points taken from 1997 onwards, a mean value of  $506 \times 10^{-15}$  is calculated with a standard deviation of  $5 \times 10^{-15}$ , which is as low as could be expected from the CS2 instability.

In the case of the CS3, the other primary clocks and one selected commercial clock were used to determine  $F_{\text{BR}}(\text{CS3})$ . Data are shown for the years during which

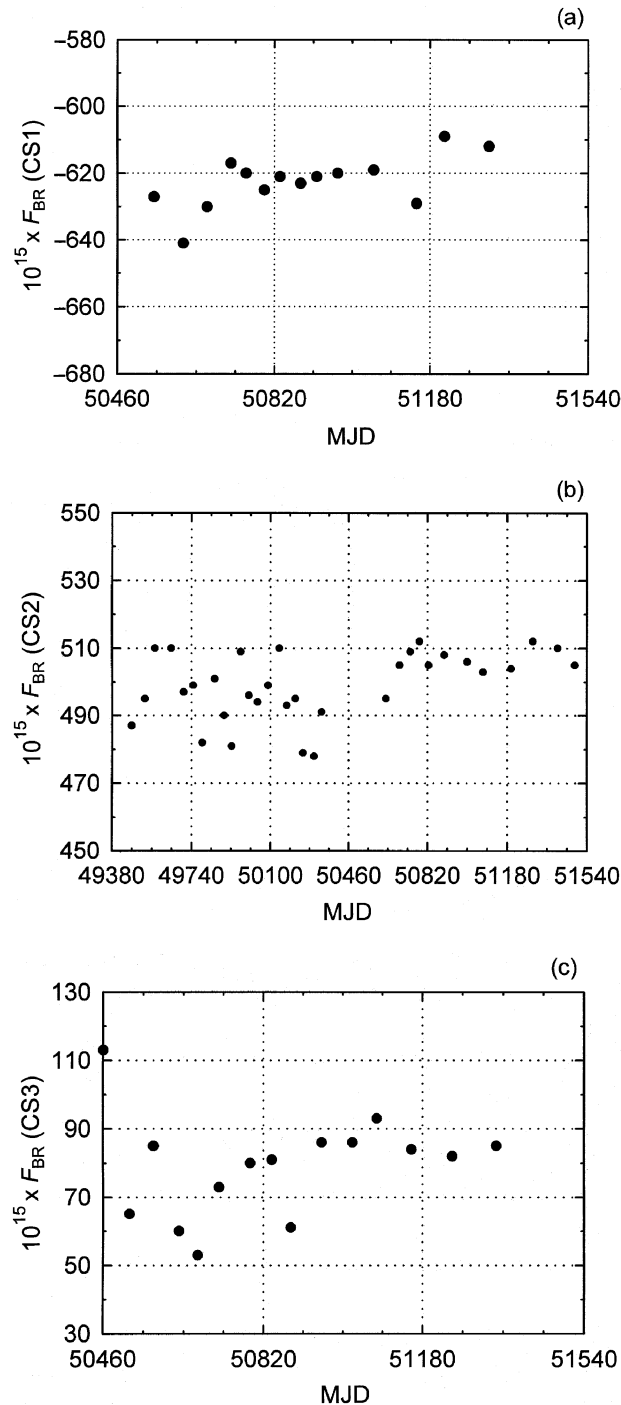


**Figure 5.** Relative beam reversal frequency shift,  $F_{BR}$ , determined for clocks (a) CS1; (b) CS2; and (c) CS3. Each data point is the difference of frequency averages with respect to reference clocks as mentioned in the text. CS1 data are shown for the period after refurbishment of the clock [6], CS2 data are shown for the last six years, CS3 data for the period during which continuous operation was achieved.

the CS3 was continuously operated. A mean value of  $F_{BR}(CS3) = 80 \times 10^{-15}$  is found with a standard deviation of  $15 \times 10^{-15}$ . No beam reversal was possible

**Table 4.** Normalized population of the Zeeman states ( $F = 4, m_F$ ) in the atomic beams of the PTB primary clocks.

| State identification $F, m_F$ | CS1 | CS2 | CS3 |
|-------------------------------|-----|-----|-----|
| 4, 1                          | 1.5 | 1.3 | 1.5 |
| 4, 0                          | 1   | 1   | 1   |
| 4, -1                         | 0.7 | 0.6 | 0.5 |

during the second half of 1999 as one detector had failed.

The results obtained for all three clocks do not give any significant indication that the previous statement of the  $u_B$  components needs to be revised.

### 5.5 Cavity pulling

All clocks have been operated at microwave power, which gives maximum clock transition signal. This power can be set with an uncertainty of 0.2 dB and has been found to be stable on all clocks within the measurement resolution. Under these conditions, the cavity pulling relative frequency shift in all clocks is below  $1 \times 10^{-16}$  [6].

### 5.6 Effect of population asymmetry (Rabi pulling, Ramsey pulling)

Frequency pulling due to the asymmetry of the neighbouring ( $\Delta F = \pm 1, \Delta m_F = 0$ ) transition lines, Rabi pulling [15], has been known for some time. Frequency shifts that cannot be explained by Rabi pulling have been explained using a new approach [16], Ramsey pulling. Both types of shift may affect the PTB primary clocks. State selection is performed using deflection of the atoms in inhomogeneous magnetic fields. As a result, the population of Zeeman states is highly asymmetrical, as can be inferred from Table 4. Rabi pulling has been avoided by operating the clocks with a relatively high magnetic field strength in the cavity region [6, 8]. Concerning Ramsey pulling, one of the present authors (BF) recently succeeded in transferring the numerical procedures from [16] to the situation prevailing in the CS1 [17] and predicted a CS1 relative frequency shift under normal operation conditions of  $-3.5 \times 10^{-15}$ . As stated in [6], no correction was applied in the case of the CS1, but an uncertainty contribution of  $3 \times 10^{-15}$  was included in the budget. Recent measurements of the CS1 dependence on the Zeeman frequency have revealed an oscillatory behaviour of the CS1 frequency with a peak-to-peak amplitude of almost  $2 \times 10^{-14}$ . These results were rather unexpected and require further study. As yet, no such experiments have been made or are planned for the CS2 and CS3. For the time being, the same uncertainty component of  $3 \times 10^{-15}$  has been included in Table 3 for all clocks.

### 5.7 Majorana transitions, microwave leakage

The entries in Table 3 for all clocks are based on experimental results obtained by power shift measurements. In this type of experiment it is difficult to distinguish between frequency shifts arising from Majorana transitions [18] and those from microwave leakage [19]. No work in this direction was undertaken in 1999, except that the level of spurious microwave fields generated from the electronic equipment, cables and feeds, was checked whenever electronic equipment was modified or replaced. In December 1999, the CS3 was dismantled and in the rf feed cable a leaking rf connector, located between the outer soft iron shield and the outer layer of the threefold Mumetal shield, was repaired. It is too early to say whether this procedure had any positive impact on clock performance.

### 5.8 Electronics: microwave spectrum, integrator offset, modulation transfer

All three clocks are operated using almost identical electronic equipment to synthesize the microwave signal for irradiating the atoms and processing the beam signal to a control voltage fed to the quartz oscillator. Basic functions of the key elements are described in [20], and the evaluation of the uncertainty components in [6] may be regarded as also valid for the CS2 and CS3. Service during the year included measurement of the microwave spectral distribution with a high-resolution rf spectrum analyser and repeated measurements of integrator offset voltage and of the detector time constant. The latter measurement has been identified as necessary to ensure proper blanking of transient components in the beam signal arising from the periodic modulation of the probing frequency [20]. The CS1 results with respect to TAI during interval A (see Table 5) were a cause of concern [14]. In fact two electronic components, the 9.2 GHz dielectric resonator oscillator and the supply of the 7 V dc voltage fed to the detector filament, which is needed to drive the caesium ions to the collector, were found to be faulty and were replaced. The CS1 again behaved normally after the replacement, but no causal relation could be identified between these two faults and the frequency excursions. The respective contribution to  $u_B$  of the CS1 (see Table 3) was increased from 1 to 10 for interval A because of these findings.

### 6. Final results

In Table 5,  $d$  designates the fractional deviation of the duration of the TAI scale interval from the SI second as realized by the individual primary clocks and is given together with the relative uncertainty contributions for specific time intervals in 1999. It is necessary to know how the uncertainties should be combined if the interval of frequency comparison required by the user is a subinterval or a combination

of the intervals of Table 5. The simplest method is to assume that the  $u_B$  components are stationary and are not reduced with increased observation time. The  $u_A$  contributions are probably reduced further below the value stated for  $\tau = 30$  d, but a monotonic decrease  $(\tau/d)^{-1/2}$  cannot be anticipated for all  $\tau$ . A previous instability analysis of the comparison between TAI and CS1, covering the period MJD 50500 to MJD 51300, showed  $\sigma_y(\tau = 60 \text{ d}) = 3.5 \times 10^{-15}$ . As normal operation of the CS1 was stopped not much later, no further analysis has been carried out. As TA(PTB) is derived directly from the CS2 without frequency steering, a comparison between TAI and TA(PTB) gives an indication of the CS2 instability in the long term. For the last 800 days (MJD 50739 to MJD 51539) one obtains  $\sigma_y(\tau = 60 \text{ d}) = 2 \times 10^{-15}$  and  $\sigma_y(\tau = 90 \text{ d}) = 1.8 \times 10^{-15}$  with a  $1 \sigma$  uncertainty of about  $6 \times 10^{-16}$  owing to the limited number of data. This result contains the model of TAI instability given above. For longer averaging times, and in the case of the CS3 for all  $\tau > 30$  d,  $u_A$  should be considered to be constant until better characterization is possible. The uncertainty component  $u_{\text{clock-TAI}}$  may be considered to be stationary ( $\approx 1 \times 10^{-15}$ ) for  $\tau > 10$  days with a small independent contribution from measurement noise (see Section 4) for shorter integration times. The uncertainty contribution from TAI,  $u_{\text{TAI}}$ , depends on the integration time  $\tau$  and is characterized by the model given in Section 4.

### 7. Conclusions

The performance of the PTB primary clocks and the uncertainty with which they have realized the SI second have been described, the final results being listed in Table 5. The current realization of TAI and time-transfer techniques make it possible to compare a sufficiently stable local frequency standard at a distant site, either through TAI or through UTC(PTB), directly with the primary clocks operated at the PTB with an uncertainty which is determined by the clocks' intrinsic  $u_B$ , provided that the interval of comparison exceeds  $\tau = 10$  days. Such a statement will no longer be valid for a comparison with the PTB caesium atomic fountain, CSF1, which should become operational during 2000; the  $u_B$  uncertainty of CSF1 has recently been evaluated as  $1.4 \times 10^{-15}$  [21].

Another observation is that the CS2 may be the most stable and reliable primary clock ever built. Data for the CS2 have been available without interruption since 1986. In 1999, the standard deviation of  $d(\text{CS2})$  in Table 5 is well below the  $u_B$  value, as expected for a well-understood primary clock. The same cannot be said of the CS3. The CS1 will probably again be useful as a primary clock in early 2000. Thus the seemingly old-fashioned primary clocks at the PTB will maintain considerable importance in the steering of TAI and thus

**Table 5.** Final results for 1999: fractional deviation,  $d$ , of the duration of the TAI scale interval from the SI second as realized by the individual clocks and uncertainty components  $u_B$ ,  $u_A$ ,  $u_{\text{clock-TAI}}$ , and  $u_{\text{TAI}}$ , all quantities in parts in  $10^{15}$ . The last two columns are common to all clocks.

| Measurement interval (MJD) | CS1                |                      |                      | CS2                |                      |                      | CS3                |                      |                      | $10^{15} \times u_{\text{clock-TAI}}$ | $10^{15} \times u_{\text{TAI}}$ |
|----------------------------|--------------------|----------------------|----------------------|--------------------|----------------------|----------------------|--------------------|----------------------|----------------------|---------------------------------------|---------------------------------|
|                            | $10^{15} \times d$ | $10^{15} \times u_B$ | $10^{15} \times u_A$ | $10^{15} \times d$ | $10^{15} \times u_B$ | $10^{15} \times u_A$ | $10^{15} \times d$ | $10^{15} \times u_B$ | $10^{15} \times u_A$ |                                       |                                 |
| A (51174-51209)            | -15                | 12                   | 5                    | -1                 | 12                   | 3                    | 39                 | 14                   | 7                    | 1                                     | 1.5                             |
| B (51209-51234)            | 2                  | 8                    | 5                    | 6                  | 12                   | 3                    | 34                 | 14                   | 7                    | 1                                     | 1.5                             |
| C (51234-51264)            | 1                  | 8                    | 5                    | 2                  | 12                   | 3                    | 39                 | 14                   | 7                    | 1                                     | 1.5                             |
| D (51264-51294)            | -1                 | 8                    | 5                    | 5                  | 12                   | 3                    | 19                 | 14                   | 7                    | 1                                     | 1.5                             |
| E (51294-51329)            | -3                 | 8                    | 5                    | -1                 | 12                   | 3                    | 27                 | 14                   | 7                    | 1                                     | 1.5                             |
| F (51329-51359)            | -4                 | 8                    | 5                    | 5                  | 12                   | 3                    | 14                 | 14                   | 7                    | 1                                     | 1.5                             |
| G (51359-51389)            | 1*                 | 9*                   | 5*                   | 3                  | 15                   | 3                    | 19                 | 20                   | 7                    | 1                                     | 1.5                             |
| H (51389-51419)            |                    |                      |                      | 8                  | 12                   | 3                    | 22                 | 14                   | 7                    | 1                                     | 1.5                             |
| J (51419-51449)            |                    |                      |                      | 3                  | 12                   | 3                    | 22                 | 14                   | 7                    | 1                                     | 1.5                             |
| K (51449-51479)            |                    |                      |                      | 10                 | 12                   | 3                    | 27                 | 14                   | 7                    | 1                                     | 1.5                             |
| L (51479-51509)            |                    |                      |                      | 8                  | 12                   | 3                    | 35                 | 14                   | 7                    | 1                                     | 1.5                             |
| M (51509-51539)            | **                 |                      |                      | 5                  | 12                   | 3                    |                    |                      |                      |                                       |                                 |

\*Interval MJD 51359 to MJD 51379.

\*\*A value was published in error in *Circular T*, issue 144.

in the realization of a well-characterized stable time scale for worldwide public and scientific applications.

## References

1. Thomas C., Wolf P., Tavella P., Time Scales, *BIPM Monographie 94/1*, 1994.
2. Thomas C., *Proc. 29th Precise Time and Time Interval (PTTI) Applications and Planning Meeting*, 1998, 19-25.
3. *BIPM Com. Cons. Temps Frequences*, 1999, **14**.
4. *Guide to the Expression of Uncertainty in Measurement*, Geneva, International Organization for Standardization, 1993.
5. Becker G., Fischer B., Kramer G., Müller E. K., *PTB-Mitt.*, 1969, **79**, 77-80.
6. Bauch A., Fischer B., Heindorff T., Schröder R., *Metrologia*, 1998, **35**, 829-845.
7. Bauch A., Dorenwendt K., Fischer B., Heindorff T., Müller E. K., Schröder R., *IEEE Trans. Instrum. Meas.*, 1987, **IM-36**, 613-616.
8. Bauch A., Fischer B., Heindorff T., Schröder R., *Metrologia*, 1996, **33**, 249-259.
9. Dudle G., Prost L., Dach R., Springer T., Schildknecht T., *Proc. 14th European Frequency and Time Forum*, 2000, in press.
10. Bauch A., deBoer H., Fischer B., Heindorff T., Schröder R., *Proc. 42nd Ann. Frequency Control Symp.*, 1988, 490-495.

11. Bauch A., deBoer H., Fischer B., Heindorff T., Schröder R., *IEEE Trans. Instrum. Meas.*, 1991, **IM-40**, 153-157.
12. Simon E., Laurent P., Clairon A., *Phys. Rev. A*, 1998, **57**, 436-439.
13. Bauch A., Heindorff T., *Proc. 8th European Frequency and Time Forum*, 1994, 503-512.
14. Bauch A., Fischer B., Heindorff T., Schröder R., *IEEE Trans. Ultrason. Ferroel. Frequ. Contr.*, 2000, **47**, 443-448.
15. De Marchi A., Rovera G. D., Premoli A., *Metrologia*, 1984, **20**, 37-47.
16. Cutler L. S., Flory C. A., Giffard R. P., De Marchi A., *J. Appl. Phys.*, 1991, **69**, 2780-2792.
17. Fischer B., *Metrologia*, 2001, **38**(3), in press.
18. Bauch A., Schröder R., *Annalen der Physik*, 1993, **2**, 421-449.
19. Dorenwendt K., Bauch A., *Proc. Joint Meeting 13th EFTF and IEEE Int. Frequency Control Symp.*, 1999, 57-61.
20. Schröder R., *Proc. 5th European Frequency and Time Forum*, 1991, 194-200.
21. Weyers S., Hübner U., Fischer B., Schröder R., Tamm Chr., Bauch A., *Proc. 14th European Frequency and Time Forum*, 2000, in press.

Received on 9 May 2000 and in revised form on 17 July 2000.